Departures from the soft collision model for Dicke narrowing: Raman measurements in the Q branch of D2

J. W. Forsman, P. M. Sinclair, A. D. May, P. Duggan, and J. R. Drummond

Citation: The Journal of Chemical Physics **97**, 5355 (1992); doi: 10.1063/1.463795
View online: http://dx.doi.org/10.1063/1.463795
View Table of Contents: http://scitation.aip.org/content/aip/journal/jcp/97/8?ver=pdfcov
Published by the AIP Publishing

Departures from the soft collision model for Dicke narrowing: Raman measurements in the Q branch of D_2

J. W. Forsman, P. M. Sinclair, A. D. May,[a] P. Duggan, and J. R. Drummond[b]
University of Toronto, Department of Physics, 60 St. George St., Toronto, Ontario, Canada, M5S 1A7

(Received 12 March 1992; accepted 7 July 1992)

With high quality spectral data, we have observed departures from the soft collision model for translational motion, in the transition region from Doppler broadening to Dicke narrowing. The departures are in agreement with theoretical calculations based on the Boltzmann equation. The implications of the results concerning the dynamics of fluids are discussed. In addition we show that the mass diffusion constant describes the translational diffusion of the optical coherence and we give precise measurements of the broadening coefficients of the $Q(0)$ to $Q(6)$ lines.

I. INTRODUCTION

It is well known that both bound state spectroscopy and the perturbation of allowed spectra by collisions can be used to explore intermolecular forces. Bound state spectroscopy is very precise, but in general explores the interaction potential only in the vicinity of the minimum. For the case of allowed spectra the dynamics of a collision probes the entire range of interaction. However it was not uncommon to have experimental errors and uncertainties in theoretical calculations of several tens of percent or larger, even as late as the early seventies. In the intervening years large advances have been made in experimental techniques, mainly due to lasers, and even larger advances in theoretical computations due to the incredible expansion in computing power. We thus find ourselves in a position to go beyond the existing semiquantitative tests, and to make a careful comparison of theory and experiment. Furthermore we now have the capability of closely scrutinizing the influence of collisions on the molecular degrees of freedom and of probing some subtle but fundamental aspects of the dynamics that have eluded experimental detection up to now. In this paper we use high resolution Raman gain spectroscopy[1,2] to take a deeper look at the influence of collisions on the translational motion of molecules in a dilute gas.

If one neglects the effect of collisions on the internal degrees of freedom then the free streaming of molecules at low densities yields the Doppler profile with a width of the order of kv, where k is the wave vector or momentum transfer and v some mean molecular speed. As is well known, the translational motion eventually takes on a random walk character at a high enough density, and the linewidth is determined by k^2D, where D is the diffusion constant. Since the diffusion constant varies as D_0/ρ, where ρ is the density in amagat units, the width decreases with increasing density, an effect known as Dicke narrowing.[3] While these simple ideas describe the spectral profile arising from the translational motion in the two limits of low and high density, to describe the spectrum at all densities one must use the space and time Fourier transform of the self-part of the van Hove pair correlation function, $G_s(r,t)$,[4,5] the probability density or distribution function for finding a molecule at position r, at time t, given that the same molecule was at the origin at $t=0$. The standard model found in the literature used to describe $G_s(r,t)$ or rather the intermediate scattering function,[6] $\chi_s(k,t) = \int e^{ik\cdot r} G_s(r,t)\, d^3r$, is the so-called soft collision model of Galatry.[7] The object of this paper is a close examination to look for departures from the soft collision model. We also address the question of whether the optical coherence diffuses at the same rate as the mass or diagonal terms of the density matrix.

The rest of this paper is organized as follows: In Sec. II we consider some underlying assumptions, particularly the manner in which the effect of collisions on the internal degrees of freedom is folded into the problem. In the third section we examine in detail, the soft collision model, the hard collision model,[8] and calculations based on solutions to the Boltzmann equation for specific intermolecular forces.[9,10] In the experimental section, measurements of the Q branch in the Raman spectrum of D_2 are presented. Following an analysis of the high density regime, the low density results are used to confirm the theoretical predictions of departures from the soft collision model. This is followed by a detailed discussion of possible systematic errors. Finally there is a summarizing paragraph of the results and some comments on the implications of our findings concerning the dynamics of fluids.

II. UNDERLYING ASSUMPTIONS

(i) We neglect collisionally induced spectral components. At low densities, the shape of a line (for an allowed transition) reflects the influence of collisions on both the translational motion and the internal degrees of freedom. Collision induced changes in the transition moment are generally small and the contribution to the spectrum spread over a range of frequency, of the order of the inverse of the duration of a collision. This is much broader than the allowed part of a spectral line and thus the collision

[a] Principal investigator with the Ontario Laser and Lightwave Research Centre.
[b] Associate of the Ontario Laser and Lightwave Research Centre.

induced spectrum forms a very low, constant background to the spectral lines and can safely be ignored or absorbed into the base line.

(ii) We assume that the temperature is sufficiently high that the translational motion may be treated classically. This means that the de Broglie wavelength is small compared to the mean distance between molecules, a condition well satisfied by D_2 at room temperature.

(iii) We assume that the effect of collisions on the evolution of the internal degrees of freedom is described by the usual list of binary collision and impact approximations.[11]

(iv) The most subtle assumption that we make is that there is no statistical correlation between the effect of collisions on the translational and internal degrees of freedom. A single collision will perturb both degrees of freedom, a condition that is necessary but not sufficient to generate a statistical correlation. In our opinion, the question of statistical correlation is not directly related to the question of speed dependent optical cross sections.[12,13] If there is no statistical correlation, then the time correlation function for the spectrum can be written as the product of two time correlation functions, one for the translational motion and one for the internal degrees of freedom; this is the true measure that the two processes are statistically uncorrelated.[14] The time correlation function for the translational motion is just the intermediate scattering function mentioned in the Introduction. For the internal degrees of freedom the usual result from binary collision theory is a time correlation function of the form $\exp(-\Gamma t)$. By itself this would lead to a Lorentzian with a half-width at half-maximum (HWHM) equal to Γ, in rad/s.

(v) Finally we assume that on times short compared to the time between collisions that the intermediate scattering function is the same as for free streaming molecules with a Boltzmann distribution of velocities.[15] This assumption will be used in the analyses of the experimental data.

Given these five assumptions it then follows that within a multiplicative factor, the experimentally observed spectrum is given by $I(k,\omega)_{\rm exp}=\int\chi_s(k,t)[\exp(-\Gamma t)]\exp(-i\omega t)dt$, where k is the difference in wave vector between the incident and scattered (stimulating) radiation. Consequently, if $I(k,\omega)_{\rm exp}$ is measured and Γ has been determined by an independent experiment, then an experimental curve for the translational correlation function, $\chi_s(k,t)_{\rm exp}$, can be extracted from the data by inversion. This may be compared to $\chi_s(k,t)_{\rm sc}$ calculated from the soft collision model. More precisely, we will examine, at a number of different densities, the residue or difference between the two, defined as $R(k,t)_{\rm exp}=\chi_s(k,t)_{\rm exp}-\chi_s(k,t)_{\rm sc}$. The thrust of the paper is to show that $R(k,t)_{\rm exp}$ is in qualitative agreement with calculations of $R(k,t)_v$ based on solutions of the Boltzmann equation[9,10] for three realistic potentials, $v\equiv$rigid sphere, $v\equiv$Lennard-Jones, and $v\equiv$exponential-six potential. We include a discussion of the hard collision model of Nelkin and Ghatak[8] since the calculations of Gibbs and Ferziger[16] imply that $\chi_s(k,T)_v$ falls between $\chi_s(k,t)_{\rm sc}$ and $\chi(k,t)_{\rm hc}$, i.e., that $0<R(k,t)_v<R(k,t)_{\rm hc}$.

III. INTERMEDIATE SCATTERING FUNCTIONS

The intermediate scattering function or spatial Fourier transform of the self-part of the van Hove pair correlation function can be expanded as a power series in $k\cdot r$,

$$\chi_s(k,t)=\int e^{ik\cdot r}G_s(r,t)d^3r$$
$$=\Sigma(-1)^n[k^{2n}]\langle r^{2n}\rangle/(2n+1)!$$
$$=\Sigma(-1)^n k^{2n}G_{2n},$$

where the isotropy of space has been used to eliminate the odd spatial moments and to establish the relationship, $\langle x^{2n}\rangle/(2n)!=\langle r^{2n}\rangle/(2n+1)!$, between the even moments of x (the component of r along k) and the even moments of r. The G's are functions of time and as defined are proportional to even powers of the molecular displacement. For example, $G_2(t)$ is $\frac{1}{6}$ the mean square displacement, $\langle r^2(t)\rangle$.

It is common in theoretical work to assume that $G_s(r,t)$ is a Gaussian function of r.[15,17] This is equivalent to stating that G_{2n} equals $(G_2)^n/n!$. The power series expansion of $\chi_s(k,t)$ then reduces to the expansion of an exponential. Resumming the series gives for the intermediate scattering function $\chi_s(k,t)=\exp(-k^2G_2)$, a function of time and Gaussian in k.[15]

We are now in a position to place the soft collision model in context. While this model has as its starting point the assumption that each collision only slightly perturbs the velocity,[16] the resulting expression for $\chi_s(k,t)_{\rm sc}$ is the same as for the Gaussian approximation. What is perhaps more important, the model yields an explicit expression for $G_2(t)$, viz. $G_2(\tau)=2(D/v_0)^2[\tau-1+\exp(-\tau)]$. Here $(v_0)^2$ is given by $2k_BT/m$ and τ is real time divided by the mean time between velocity changing collisions, itself given by, $\tau_0=2D/(v_0)^2$. In the short time limit G_2 or $(1/6)\langle r^2\rangle$ approaches the free streaming limit of $(v_0t/2)^2$. In the long time limit G_2 goes to the well known random walk value, Dt. The origin of this form of G_2 can be traced at least as far back as Doob.[18] Here we spot a slight conceptual inconsistency in the soft collision model; τ_0 is related to the diffusion constant, as given by the equation above, but the diffusion constant in a dilute gas is usually considered to measure the hard core of molecular interactions, not distant, soft, collisions that only slightly change the velocity. It would be more informative to describe the "soft collision model" as one based on the Gaussian approximation *and* a form of G_2 that has the correct short and long time behavior. We will return to a discussion of the form of G_2 in Sec. VII and to a discussion of the Gaussian approximation in the concluding section of the paper. We now consider *departures* from the soft collision model.

Starting from the Boltzmann equation it is possible to evaluate numerically the even moments of the molecular displacement. Desai[9,19] and Desai and Nelkin[10] have calculated these up to the eighth moment for a rigid sphere, a Lennard-Jones and an exponential-six potential. In a private communication, Desai claims that his numerical values of G_2 were very close to G_2 for the soft collision model,

provided τ_0 was defined as above and D was calculated directly from the intermolecular potential.[20] Thus deviations from the soft collision model are found in the higher spatial moments. In Refs. 9 and 10 there are plots of $[G_{2n}]_v/[G_{2n}]_{sc}$, ($n=1$, 2, and 3) from which the non-Gaussian corrections to the fourth, sixth, and eighth moment may be calculated, i.e., from the plots we can determine the first three terms of the spatial moment expansion of the residue, $R(k,t)_v$, for three intermolecular potentials.[21]

The hard collision model of Nelkin and Ghatak[8] assumes that the molecular velocity is completely thermalized in a single collision. For the hard collision model $\chi_s(k,t)$ may be calculated from the analytic expression for $S(k,\omega)_{hc}$. By numerically transforming $S(k,\omega)_{hc}$, we can generate $\chi_s(k,t)_{hc}$ and from this the residue for the hard collision model, $R(k,t)_{hc}=\chi_s(k,t)_{hc}-\chi_s(k,t)_{sc}$. This is the complete residue, not a truncated moment expansion.

In summary, there exist in the literature, *theoretical* graphs from which the first three terms of $R(k,t)_v$ for a Lennard-Jones, exponential-six and a rigid sphere potential may be calculated and it is possible to calculate the full $R(k,t)_{hc}$ for the hard collision model. The only parameter that we need to specify to carry out the calculations of $R(k,t)_v$ or to determine $R(k,t)_{hc}$, is the diffusion constant, D.

To extract the *experimental* residue from the spectral profiles, we need the measured spectrum, $I(k,\omega)_{exp}$, the diffusion constant, D, and the broadening parameter, Γ. In Sec. IV we will show how it is possible to determine these two crucial parameters from the spectral data at high density without biasing the extraction of the residue from the spectral data at lower densities. In the discussion we will establish that this method of analysis is essential to obtain a physically consistent picture.

IV. EXPERIMENTAL METHOD AND OBSERVATIONS

The high resolution Raman gain spectrometer[1,2] used a tunable dye laser as the Raman probe and an argon ion laser as the Raman pump. Raman gain spectroscopy was used since it measures the imaginary part of the third order susceptibility directly without interference from the dispersion.[22] Relative frequencies were measured with a scanning Fabry–Perot interferometer which yielded a precision (reproducibility) of 1–2 MHz. The instrumental linewidth is $\sim$1.5 MHz (Ref. 23) and is $<1\%$ of the narrowest line width measured. It is limited by the pump and probe lasers both of which are frequency stabilized. At any given density the shape of the line was measured at least twice, using a scan of 30 GHz (1.0 cm^{-1}) centered on the line. The deuterium gas (Matheson C. P. grade, 99.5% pure) was contained in a cell $\sim$20 cm long and temperature controlled at 30.2 °C. A capacitance pressure transducer (MKS Baratron, model 390 HA), a calibrated thermocouple, and PVT data[24] were used to determine the density. An accuracy of 0.16% was achieved above $\sim$0.6 amagat.[25] Below 0.6 amagat the accuracy decreased to $\sim 1\%$ at the lowest density, due to temperature induced drifts in the zero of the pressure transducer. At densities >2 amagat, the signal to noise for the $Q(2)$ line exceeded 1700 with (i) a one second integration time; (ii) 200 mW in the probe beam; (iii) 540 mW peak-to-peak modulation for the pump; and (iv) in a single pass configuration. Within the accuracy of our measurement, the spectrometer performs at or very close to both the theoretical signal and shot noise limit.

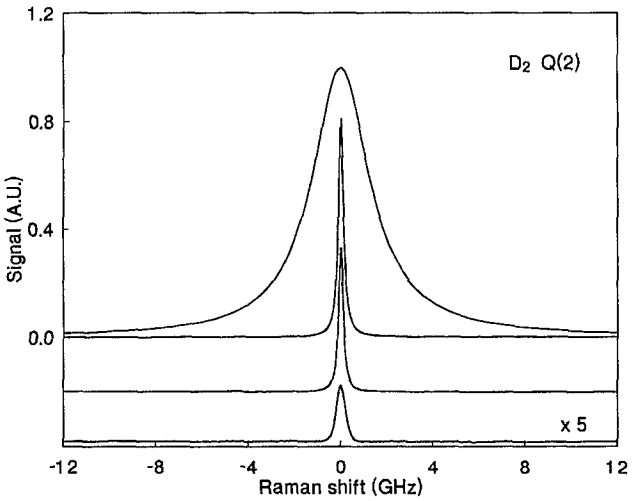

FIG. 1. The $Q(2)$ line of D_2 at 30.2 °C and from top to bottom, 23.92, 1.525, 0.979, and 0.102 amagat units of density. The base lines for the two lowest densities have been offset.

The $Q(0)$, $Q(1)$, and $Q(3)$ lines were measured at many densities from 0.2 to 24 amagat. The strongest line $Q(2)$ was measured from 0.1 to 24 amagat. For integration times of 4 s, the signal to noise ratio for the lowest densities was $\sim$200. While not central to this paper, we also measured the broadening of the $Q(4)$, $Q(5)$, and $Q(6)$ lines from 3.4 to 28 amagat.[26]

Figure 1 shows the $Q(2)$ line at several densities. For the purpose of illustration, the discrete data points have been joined by straight line segments and the centers of the lines for different densities have been aligned. That there is a minimum in the width as a function of density, is evident from an examination of the curves. This is true for all the lines examined. Figure 2 shows the HWHM (measured in GHz) as a function of density, for the four strongest lines. The error bars, vertical or horizontal, are much less than the size of symbols for the points, even less than the width of the solid lines. The insert shows the low density data on an expanded scale; it is in this region that the calculations predict a departure from the soft collision model. The reason for recording the high density data was to determine D and Γ.

If we accept the basic assumptions outlined above then theory predicts a Doppler broadened line at low density, a transition region from a Doppler broadened line to a Dicke narrowed line, with finite departures from the soft collision model, and a high density regime where the soft collision model is applicable. The latter is equivalent to stating that the line will be Lorentzian with a HWHM (in rad/s) given by $\Delta\omega=k^2D+\Gamma$. The transition region occurs around the

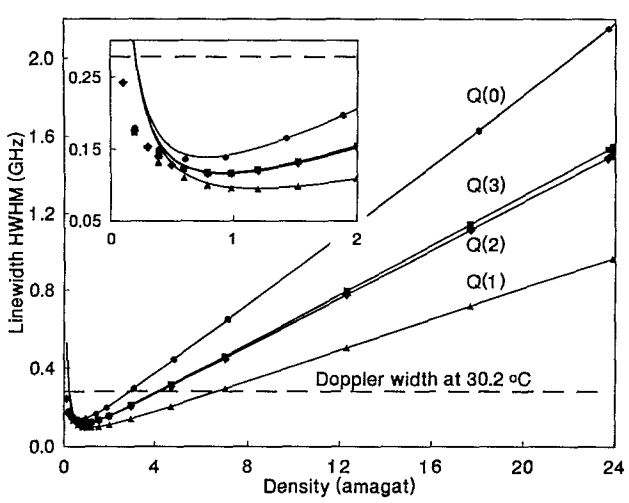

FIG. 2. Linewidths as function of density for the $Q(0)$–$Q(3)$ line in D_2.

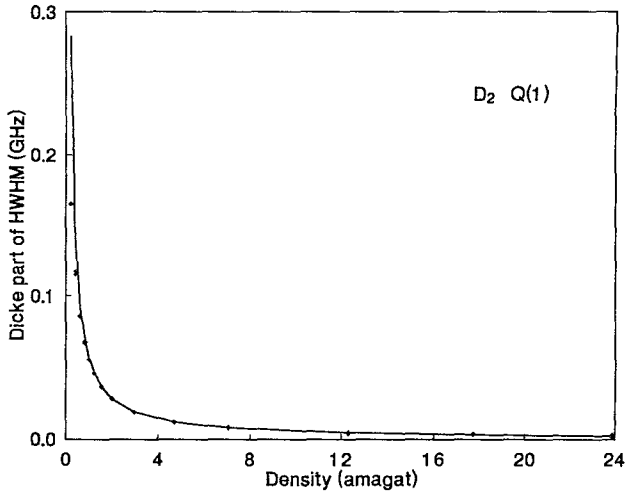

FIG. 3. Contribution of the translational motion to the width of the $Q(1)$ line.

density for which $k\Lambda=1$, where Λ is the mean free path. For the Q branch of D_2 and forward scattering, the corresponding density is ~ 0.4 amagat. The question is "Do the observations support all the predictions?" We begin by analyzing the high density regime.

V. DETAILED ANALYSES (HIGH DENSITY)

For the Q branch lines in D_2, high density means densities (much) greater than 0.4 amagat. To first order, the line shape in this region, should be Lorentzian with a HWHM given by $k^2D_0/\rho+B\rho$. Here we have inserted the inverse density dependence of the diffusion constant, D, and the linear dependence on density of the collision broadening, Γ. Such an expression fits the measured widths very well for all densities down to ~ 1 amagat. Essentially, the solid lines in Fig. 2 are the best fit curves of this form, where only the data above 1.4 amagat were used to determine D_0 and B. If one includes densities below 1 amagat the quality of fit deteriorates and the value of D_0 extracted from the fit decreases rapidly. In addition there are observable departures of the calculated Lorentzian line shape from the experimental line shape. To illustrate the contribution of the translational motion to the $Q(1)$ linewidth, we have plotted in Fig. 3 the measured HWHM minus the calculated value of $B\rho$, where B is a best fit value, and compared the points to the best fit value k_2D_0/ρ. The fit is excellent above 1.4 amagat. The departure of the points from the solid line below ~ 1 amagat is consistent with the arguments and estimates given above. At 24 amagat the translational width is 2.5 MHz which is small compared to the collisional width of ~ 1000 MHz. Near 1 amagat the collisional width has fallen from 1000 to ~ 50 MHz while the diffusional width has risen from 2.5 to 50 MHz. (The minimum in the curves shown in Fig. 2 occurs when the two contributions are equal.) The point of Fig. 3 is that we can detect a contribution of the translational motion to the width of a line over a wide range of density, which is *essential* if one wants a precise value of D_0 (and B). For maximum precision, the density range must start just above the transition density. It is the results of the analyses at high densities that permit us to look for departures from the soft collision model at the low densities corresponding to the insert in Fig. 2.

Before proceeding to the low density data we examine the validity of the two assumptions made in the last paragraph, namely that D varies as D_0/ρ and Γ as $B\rho$. The Enskog theory of dense gases predicts that D should be given to the lowest order of correction as, $D_0/\rho-5\pi L\sigma^3/12$, where L is Lodschmidt's number and σ the hard sphere diameter.[20] Using $\sigma=2.95\times10^{-8}$ cm (Ref. 20) we calculate the additional width due to the constant correction to D, as -0.05 MHz. This is very much smaller than our instrumental width, which itself is just at our level of detection. Thus dense gas corrections to the diffusion constant may be neglected. For the broadening, Royer[27] has predicted a density dependence of, $\Gamma=B\rho+B'\rho^3$. The high density correction arises because the duration of a collision is no longer negligibly small compared to the time between collisions. With a fixed D_0, B, and B' we were able to fit the measured half-widths (above 1.4 amagat) to within ± 2 MHz. (In Fig. 3 the data points are actually the experimental half-widths minus $B\rho+B'\rho^3$]. Table I lists the values of D_0, B, and B' and the values of D_0 and B if B' is set equal to zero in the fitting routine, for $Q(0)$, $Q(1)$, $Q(2)$, and $Q(3)$. Also included are some preliminary broadening coefficients for the weak lines $Q(4)$, $Q(5)$, and $Q(6)$ and the very approximate values of D_0 determined from these lines.

There are three pieces of evidence that support the inclusion of a cubic term in the effect of collisions on the internal degrees of freedom. Including a cubic term in the fit (i) marginally improved the quality of the fit of the width vs density; (ii) decreased the variation of the fitted value of D_0 from one Q branch line to the next (one expects a negligible dependence of D on rotational quantum number); and (iii) decreased the sensitivity, of the value of D_0 deduced, to both the lower and the upper end of the range

TABLE I. Experimental broadening coefficients and D_0 for the Q branch lines of D_2 at 30.2 °C, with and without allowance for nonlinear broadening. Note the units for B and B'. The quoted errors do not include the possible systematic errors associated with the calibration of the density and frequency scales.

Line	B (MHz/amagat)	B' (kHz/amagat^3)	D_0 (cm^2 amagat/s)
$Q(0)$	90.43(11)	0.0	0.816(86)
	89.38(10)	2.30(22)	0.954(35)
$Q(1)$	40.30(02)	0.0	1.000(12)
	40.44(04)	−0.30(7)	0.985(09)
$Q(2)$	62.71(03)	0.0	0.943(30)
	62.60(11)	0.22(18)	0.955(32)
$Q(3)$	64.40(04)	0.0	0.927(31)
	64.14(10)	0.54(18)	0.958(28)
$Q(4)$	64.4(2)	0.0	0.99(30)
$Q(5)$	51.6(1)	0.0	0.99(10)
$Q(6)$	38.4(1)	0.0	0.82(18)

of densities included in the fit. Including a B' term changed the fitted values of B by $\sim 1\%$ for the broadest line, $Q(0)$, and $\sim 0.2\%$ for the others.

From the least-squares fit, the uncertainty in D_0 determined for each line varied from 0.009 to 0.035 cm^2 amagat/s. Within experimental error, our values of D_0 agree with the value of 0.979(17) cm^2 amagat/s derived from a critical compilation,[28] and reports of binary diffusion of D_2 into H_2 (Refs. 29, 30, 31) and para-H_2 into n-H_2.[32] They also agree with the values determined by Smyth *et al.*[33] This suggests that the "optical" or coherence diffusion constant[34] is not distinct from the mass diffusion constant. In other words, the coherence involved in the scattering is fixed to the molecule so that the population (mass) transport of the molecule also accounts for the translational part of the optical coherence. The mean value of D_0 determined from our measurements is 0.963(14) cm^2 amagat/s.

VI. DETAILED ANALYSES (LOW DENSITY)

Having determined the broadening coefficients and the diffusion constant from the high density data, the next step was to extract the experimental translational correlation function from the spectra at low densities. This was accomplished by taking the fast Fourier transform (FFT) of the spectra[35] and dividing by $\exp[-(B\rho+B'\rho^3)t]$, where in actual practice, at low densities, the cubic term was totally negligible. Next we computed the correlation function of the soft-collision model using our mean experimental value of D_0. Finally we calculated the residue, $R(k,t)_{\text{exp}}$, or the experimental translational correlation function minus $\chi_s(k,\tau)_{\text{sc}}$, for the soft collision model. Figures 4(a), 4(b), and 4(c) show this residue, as a function of τ, for the $Q(2)$ line at 0.196, 0.394, and 0.599 amagat, respectively. We see that the residue vanishes at very short and very long times, as predicted[9,10,19] (however, see below). At the lowest density and intermediate times, $\tau \simeq 5$, the magnitude of the residue is of the order of a few percent.[36] The residue is zero, within the noise limit set by our transforms, at 0.6 amagat and higher densities. The same results were found for the other lines but with a slightly higher level of noise.

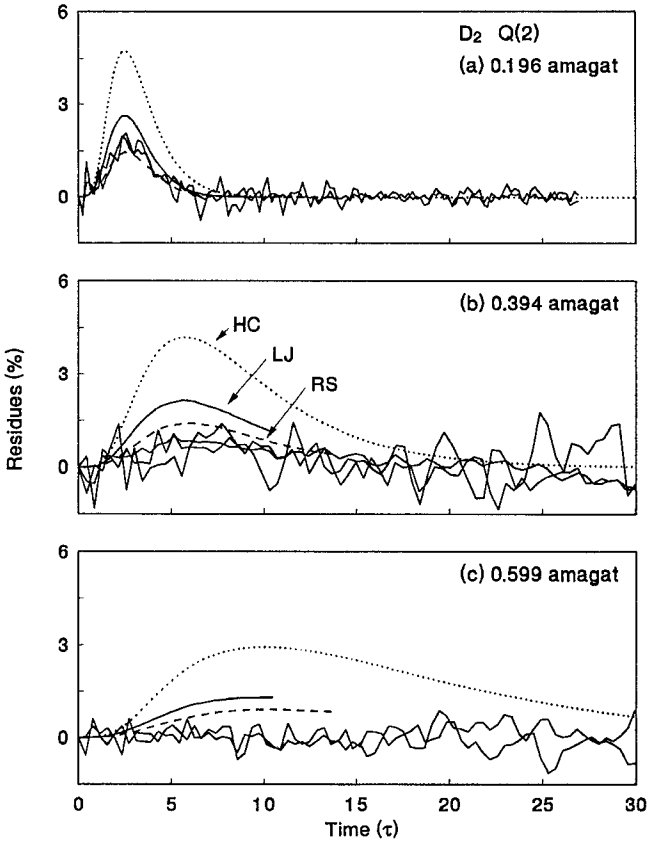

FIG. 4. Experimental residues for the $Q(2)$ line and those calculated from the hard collision model (HC), rigid sphere interaction (RS), and the Lennard-Jones potential (LJ). The plot for the exponential-six potential is almost the same as for the Lennard-Jones. Multiple traces at a given density correspond to separate measurements of the line shape.

For a single trace of the $Q(0)$ line, a small residue, just above the noise limit, was observed at 0.6 amagat.

We cannot make a direct comparison of our experimental results with the moment expansion, as such a series converges rather slowly. However, Desai[19] has shown how to reorder the series in a manner that converges rapidly. Using this form and his graphs[21] we have determined the residue for a rigid sphere potential (RS) in Fig. 4 and a Lennard-Jones potential (LJ) in Fig. 4. The residue for an exponential-six potential is very close to that for a Lennard-Jones potential and is not shown separately in the figures. Also shown in the figures is the residue for the hard collision model of Nelkin and Ghatak.[8] We remind the reader that zero residue corresponds to the translational motion being described by the soft collision model. We see that the hard collision model of Nelkin and Ghatak considerably overestimates the non-Gaussian corrections. The residues are best described by solutions of the Boltzmann equation.[37] While the experimental values of the residue lie closest to the values calculated for hard spheres, we cannot claim unequivocally that a hard sphere potential is best for a description of departures of the translational motion from that given by the soft collision model; the calculations were done at 95 K not 303 K.[38] Low temperatures emphasize the difference between a rigid sphere and potentials

with an attractive part. To bring out the difference it would be better to repeat the experiments at liquid nitrogen temperatures. Nevertheless, we can conclude that both the magnitude and the time scale of the observed residue agree with the calculations of Desai[9,19] and Desai and Nelkin.[10] What remains is to examine the influence of systematic errors on our experimental results and on the calculated residues.

VII. POSSIBLE SYSTEMATIC ERRORS

We find the lines are very slightly asymmetric. This may be due to "other" or induced focusing,[1,2] an intrinsic asymmetry[12] or to line mixing effects.[39] The asymmetry is neglected in the FFT since we retained only the real part. However the amount of asymmetry and thus the size of both the real and imaginary part of the FFT depends upon the choice of line center. Refitting the lines, but including a dispersion curve to account for an asymmetry, changed the position of the line centers at the three lowest densities by <2 MHz. Adjustments of the line center by 2 MHz modified the residue extracted from the data by $<0.1\%$ or much less than the RMS noise in the experimental residues.

The residue was quite sensitive to the value of B at densities *above* 0.5 amagat. A change in B by 0.5% generates a significant residue. This is hardly surprising since one is wrongly describing the broadening which is becoming the dominant contribution to the linewidth at these densities. The error carries through to a compensating but incorrect description of the translational motion. Our analysis rests heavily on the premise that the high density limit is correctly described by the usual simple picture of Dicke narrowing and collision broadening, in which case the residue vanishes at high densities. Our results are consistent with such behavior since our best fit values of B and D_0 yield zero residue within the noise. At *low densities* (below 0.5 amagat) the residue was insensitive to small changes in B. This is the very reason for having chosen D_2 as the test gas. There is little broadening at densities for which one anticipates departures from the soft collision model.

Since the integral under the line determines the zero time value of the correlation function, the choice of base line strongly influences the very short time behavior of the experimental translational correlation function. (To a much lesser extent, it also affects the size of the function at all times since we normalize every correlation function to unity at $\tau=0$.) Below 1.5 amagat the spectrum falls off more rapidly than a Lorentzian so it is easy to observe far enough into the wings to determine the base line accurately. Occasionally we corrected the base line by an amount of the order of the noise on the spectrum to make the residue go to zero smoothly at short times. At the lowest density, where the residue is the largest, provided we stayed within the limits set by the noise, varying the background did not influence the calculated residue except at very short times ($\tau<1$) where theory and the models are all unambiguous; the residue should go to zero. Around 0.6 amagat base line adjustments do influence the residue. This probably explains the variations we have observed from one run to another.

The largest influence on the residue (but still small) came from the diffusion constant used to calculate the soft collision model. At densities of 0.4 amagat and higher, adjustments, within our estimated error on the mean value of D_0 (± 0.014 cm^2 amagat/s), resulted in changes to the residue of the same order as the noise shown in the figure. Note however, there is a trap here for the experimentalist. It is possible at each density to choose a diffusion constant that generates zero residue, i.e., to artificially drive the experimental data into agreement with the soft collision model. The D so derived will be lower than the mass diffusion constant. If one examines only a limited range of densities one might conclude that the soft collision model correctly describes the spectra but the optical coherence diffuses more slowly than the diagonal elements in the density matrix. However, if a large range of densities is explored, the density dependence of the diffusion constant will not match the known density dependence, $D=D_0/\rho$. Our approach has been to make measurements over a large range of density and to seek a unified and consistent interpretation of the results over the entire range.

The uncertainty in the measurement of the density affects the values of $D=D_0/\rho$ and $\Gamma=B\rho+B'\rho^3$ used to extract the residue from the spectral profile. Within the estimated uncertainties any error in the density has a negligible effect on the $R(k,t)_{\rm exp}$ at densities at or below 0.4 amagat, and a small influence around 0.6 amagat.

Finally we considered two other possible sources of systematic error. (i) Calculation[40] showed that the 1.5 MHz finite resolution of the spectrometer could be ignored even for the narrowest line ($\Gamma=90$ MHz, HWHM) and (ii) linewidth corrections that one introduces, if one simply applies the work of Dattagupta and Turski,[41] is smaller than the already negligible finite resolution of the spectrometer.

We are not aware of any other possible sources of systematic errors. Thus overall, provided we accept the limiting spectral behavior at high densities, it is not possible to dismiss the residue as arising from biases in the experiment.

There are biases in the residues computed from the literature.[21] Desai has not given the actual G_2, for any of the potentials. Thus in constructing $R(k,t)_v$ we have used the soft collision form of G_2. This introduces a systematic error into the calculated residues which, at least in the case of a rigid sphere, we can show to be small. The relation between G_2 and the velocity–velocity correlation function is given by $\langle \bar{v}(t)\cdot\bar{v}(0)\rangle = 3d^2G_2/dt^2$. The soft collision model form of G_2 is equivalent to an exponentially decaying velocity–velocity correlation function. This is not exact however and for rigid spheres we can quantify the deviations from an exponential. Desai and Ross[43] have given in their Fig. 3 departures of the velocity–velocity correlation function from an exponential. We have found empirically that the function, $0.1\tau^2\exp[-\tau]$ fits their curve, of departure from an exponential decay, remarkably well. On integrating the total velocity–velocity correlation function we

find a new G_2 for rigid spheres that is given by $G_2(\tau)_{rs} = 2[D/(1.02)v_0]^2 \{[\tau-1+\exp(-\tau)]+0.1[(\tau^2+4\tau+6)\exp(-\tau)+(2\tau-6)]\}$, where the new τ_0 is given by $\tau_0 = 2D/(1.02)v_0^2$. By direct comparison at equal times and at a density of 0.2 amagat we find that the maximum difference between G_2 for the soft collision model and for the rigid sphere amounts to only 0.6% for τ about 2.5. Of course the difference vanishes at very short and very long times. When this new G_2 is combined with the plots of Desai[21] to generate what is presumably the exact residue for a rigid sphere, we find a value of $R(k,t)_{RS}$ 10% higher at the peak and even closer to the experimental curves. We conclude from this, as implied throughout the paper, that the experiment is more a check on the Gaussian approximation, than on the form of G_2.

VIII. SUMMARY AND COMMENTS

In summary, for D_2 at room temperature.

(1) With five basic assumptions, we have shown that it is possible to give a complete description of an isolated line from the free streaming to the collision broadened, completely Dicke narrowed regime.

(2) We have measured departures from the soft collision model in the transition region from free streaming to Dicke narrowing and shown for low density gases that the translational motion is described by solutions of the Boltzmann equation. Because the corrections are small, one can also turn this around. In situations requiring the modeling of a complete and complicated spectrum such as for the upper atmosphere, the soft collision model provides a reliable line shape for computing the contribution of a single line to the complete spectrum. Of course line interference effects or motional narrowing[42] may invalidate a simple line additive model for certain regions of complex spectra.

(3) We have shown for room temperature D_2, that the optical coherence diffuses at the same rate as the population (mass).

(4) We have determined very precise broadening coefficients. The latter can be used in critical tests of collision broadening theory.

To the best of our knowledge this is the first time that spectroscopy has been used, in depth, to explore the self-part of the van Hove pair correlation function in a low density regime where a binary collision solution to the Boltzmann equation is valid. However before one can use this type of spectroscopy to measure the isotropic part of intermolecular potentials, we feel that the important question of the correlation of the effects of collisions on the translational and internal degrees of freedom must be addressed. The question of nonlinear broadening at high densities should also be explored.

This work has implications for the theory of fluids. $G_2(t)$ for the hard and soft collision model are identical. It is also of the same form for a combination of the hard and soft collision model.[16] We have noted above that there is only a small difference between G_2 for a rigid sphere and the soft collision model. Thus *there is a dynamical scaling law operating in low density gases.* The mean square displacement of a molecule in a fluid, for any intermolecular interaction, is given say within a percent by, $(1/6)\langle r^2(\tau)\rangle = G_2(\tau) = 2(D/v_0)^2[\tau-1+\exp(-\tau)]$, where τ is t/τ_0, τ_0 is given by $\tau_0 = 2D/v_0^2$, and D is to be calculated from the intermolecular potential using the standard approach.[20] This scaling law is not surprising given the relationship between G_2 and the velocity–velocity correlation function; it is well known that random collisions produce exponential decays.[43,44]

This dynamical scaling takes on greater importance if the self-part of the van Hove correlation function, $G_s(r,t)$, is Gaussian in r. At low densities, where correlations created by molecular collisions may be ignored, the Boltzmann distribution of velocities guarantees a Gaussian distribution.[17] At high densities, if there are a very large number of molecules in the volume being probed by the experiment, i.e., a volume of linear dimension (much) less than $1/k$, in the Raman experiments of this paper, and the correlation length, $\sim \sqrt{Dt}$, is smaller than this size, then, neglecting slow hydrodynamic modes, the volume sampled may be subdivided into smaller volumes that are statistically independent. In this case the central limit theorem[14] again allows us to conclude that the van Hove function $G_s(r,t)$ is again Gaussian. Being correct in the limit of low and high densities, then a reasonable first order theory is to assume that $G_s(r,t)$ is Gaussian at all densities. This is the reason the soft collision model works so well. The departures from the soft collision model reported here may be interpreted as departures from dynamical scaling in the sense of Yip.[45]

ACKNOWLEDGMENTS

This research was supported by the Natural Sciences and Engineering Research Council of Canada and the Government of Ontario through the Ontario Laser and Lightwave Research Centre. Two of the authors (J.W.F. and P.M.S.) acknowledge Walter C. Sumner Memorial Fellowships. The authors would like to acknowledge the very fruitful discussions with R. C. Desai on the statistical mechanics aspects of this paper.

[1] J. W. Forsman, P. M. Sinclair, P. Duggan, J. R. Drummond, and A. D. May, Can. J. Phys. **69**, 558 (1991).
[2] Jon Forsman, Ph.D. thesis, University of Toronto, 1992.
[3] R. H. Dicke, Phys. Rev. **89**, 472 (1953).
[4] L. van Hove, Phys. Rev. **95**, 249 (1954).
[5] V. G. Cooper, A. D. May, E. H. Hara, and H. F. P. Knaap, Can. J. Phys. **46**, 2019 (1968).
[6] The self-part of the intermediate scattering function is the spatial Fourier transform of the self-part of the van Hove pair correlation function, $G_s(r,t)$, and is often used in describing neutron scattering.
[7] L. Galatry, Phys. Rev. **122**, 1218 (1961).
[8] M. Nelkin and A. Ghatak, Phys. Rev. **135**, A4 (1964).
[9] R. C. Desai, J. Chem. Phys. **44**, 77 (1966).
[10] R. C. Desai and M. Nelkin, Nucl. Sci. Eng. **24**, 142 (1966).
[11] P. R. Berman, Appl. Phys. **6**, 283 (1975).
[12] R. L. Farrow, L. A. Rahn, G. O. Sitz, and G. J. Rosasco, Phys. Rev. Lett. **63**, 746 (1989).
[13] P. R. Berman, J. Quantum Spectrosc. Radiat. Transfer **12**, 1331 (1972).
[14] L. E. Reichl, *A Modern Course in Statistical Physics* (University of Texas, Austin, 1980).
[15] At low densities the self-part of the van Hove correlation function will go to that of an ideal gas. For an ideal gas (free streaming molecules)

$\bar{v}=\bar{r}/t$ so that $G_s(r,t)=[\pi(v_0t)^2]^{-3/2}\exp[-r^2/(v_0t)^2]$ and has the cannonical Gaussian form $[\pi\omega^2(t)]^{-3/2}\exp[-r^2/\omega^2(t)]$. The corresponding, low density, intermediate scattering function is $\chi_s(k,t)=\exp-[kv_0t/2]^2$. The soft collision model goes to the same expression at short times.

[16] A. G. Gibbs and J. H. Ferziger, Phys. Rev. **138**, 701 (1965).

[17] G. H. Vineyard, Phys. Rev. **110**, 999 (1958).

[18] J. L. Doob, Ann. Math **43**, 351 (1942).

[19] R. C. Desai, Ph.D. thesis, Cornell University, 1966). See also R. C. Desai and M. Nelkin, Phys. Rev. Lett. **16**, 839 (1966).

[20] J. O. Hirschfelder, C. F. Curtis, and R. B. Bird, *Molecular Theory of Gases* (Wiley, New York, 1954).

[21] We are indebted to R. C. Desai for making the large original plots of the non-Gaussian corrections available to us.

[22] A. Owyoung, Opt. Commun. **22**, 323 (1977). The statements made in this reference, concerning the real and imaginary parts of the third order susceptibility, are correct in the plane wave limit. However, for Gaussian beams induced focusing (see Refs. 1 and 2) can make the signal sensitive to the dispersion associated with the Raman gain. This is the two color Raman equivalent to the "two color Z scan" of Van Stryland, Opt. Lett. **17**, 258 (1992).

[23] For resolution we give the RMS width. For all other widths in this paper we give the half-width at half-maximum.

[24] A. Michels, W. de Graaff, T. Wassenaar, J. H. M. Levelt, and P. Louwerse, Physica **25**, 25 (1959).

[25] 1 amagat is the density at 0 °C and 1 atm and corresponds to 22 433 cm^3/mol for D_2.

[26] The preliminary values for B reported in Ref. 1 are incorrect due to a mislabeling of the type of thermocouple wire used to measure the temperature of the cell.

[27] A. Royer, Phys. Rev. A **22**, 1625 (1980).

[28] T. R. Marrero and E. A. Mason, J. Phys. Chem. Ref. Data **1**, 3 (1972).

[29] P. J. Dunlop, C. M. Bignell, W. L. Taylor, and B. A. Meyer, J. Chem. Phys. **87**, 3591 (1987).

[30] A. S. M. Wahby, A. J. H. Boerboom, and J. Los, Physica **74**, 85 (1974). They do not state explicitly the reference temperature used for converting their relative measurements to absolute values. We used only their temperature dependence in scaling the data from other papers.

[31] K. P. Müller and A. Klemm, Z. Naturforsch. Teil A **25**, 243 (1970).

[32] P. Harteck and H. W. Schmidt, Z. Phys. Chem. **21B**, 447 (1933).

[33] K. C. Smyth, G. J. Rosasco, and W. S. Hurst, J. Chem. Phys. **87**, 1001 (1987).

[34] P. L. Varghese and R. K. Hanson, Appl. Opt. **23**, 2376 (1984).

[35] For the FFT we used a local smoothing routine to generate a data file at equal frequency steps.

[36] $\chi_s(k,\tau)$ is normalized to 1 at $\tau=0$. Thus a residue of 0.03 is only 3% of the peak value of $\chi_s(k,\tau)$. We have plotted all residues as a percentage.

[37] Technically speaking the soft and hard collision models can be considered to be solutions of the Boltzmann equation. Here however, by solutions to the Boltzmann equation we mean solutions where the collision integral is actually evaluated for a specific intermolecular potential.

[38] The difference between the Lennard-Jones and the rigid sphere results is most likely due to the fact that the scattering and thus the diffusion for the Lennard-Jones potential are temperature dependent. For D_2 at 303 K, where the experiments were performed, the attractive part is insignificant compared to the hard core part. However Desai's calculation was done for 95 K where the attractive part of the Lennard-Jones interaction plays a greater role.

[39] P. W. Rosenkranz, IEEE Trans. Antennas Prop. **AP-23**, 498 (1975).

[40] A. K. Arora and V. Umadevi, Appl. Spectrosc. **36**, 424 (1982).

[41] S. Dattagupta and L. A. Turski, Phys. Rev. A **32**, 1439 (1985).

[42] T. Witkowicz and A. D. May, Can. J. Phys. **54**, 575 (1976).

[43] The simplest example relevant to the present work is of course the damping of the internal degrees which leads to the collision broadening.

[44] J. Dalibard, Y. Castin, and K. Molmer, Phys. Rev. Lett. **68**, 580 (1992).

[45] S. Yip, Annu. Rev. Phys. Chem. **30**, 547 (1979).